Dinuclear Spin Cross-Over Complexes Based on Tetradentate and Bridging Cyanocarbanion Ligands

Journal:	*Inorganic Chemistry*
Manuscript ID	ic-2016-01542f
Manuscript Type:	Article
Date Submitted by the Author:	28-Jun-2016
Complete List of Authors:	Milin, Eric; Universite de Bretagne Occidentale, UMR CNRS 6521 Belaid, Sabrina; Universite de Bejaia Patinec, Veronique; Université de Brest, Laboratoire de Chimie, Electrochimie Moléculaires et Chimie Analytique, UMR CNRS 6521 Triki, Smail; Universite de Bretagne Occidentale, Chimie, Electro. Molecularies et Anal. Chastanet, Guillaume; CNRS, ICMCB Marchivie, Mathieu; Universite de Bretagne Occidentale, UMR CNRS 6521

Dinuclear Spin Cross-Over Complexes Based on Tetradentate and Bridging Cyanocarbanion Ligands.

Eric Milin,[†] Sabrina Belaïd,[†,§] Véronique Patinec,[†] Smail Triki,[*,†] Guillaume Chastanet,[‡] Mathieu Marchivie[‡]

[†]UMR CNRS 6521, Chimie, Electrochimie Moléculaires, Chimie Analytique, Université de Bretagne Occidentale, 6 Avenue V. Le Gorgeu, BP 809, 29285 Brest Cedex, France.
[§]Laboratoire de Physico-chimie des Matériaux et Catalyse, Université de Béjaia, Algeria.
[‡]CNRS, Université Bordeaux, ICMCB, 87 Av. Doc. A. Schweitzer, F-33608 Pessac, France.

ABSTRACT: Spin-crossover (*SCO*) Fe(II) dinuclear complexes of formula $[Fe_2(tmpa)_2(\mu_2\text{-}tcpd)_2]\bullet 0.8(CH_3OH)$ (**1.MeOH**) and $[Fe_2(andmpa)_2(\mu_2\text{-}tcpd)_2]\bullet 2CH_3OH$ (**2.MeOH**) (tmpa = tris(2-pyridylmethyl)amine, andmpa = bis-(2-pyridylmethyl)aminomethyl)aniline, $(tcpd)^{2-}$ = 2-dicyanomethylene-1,1,3,3-tetracyanopropanediide) have been synthesized and characterized by infrared spectroscopy, X-ray diffraction and magnetic measurements. The crystal structure determinations of the two complexes (**1.MeOH** and **2.MeOH**) and the desolvated complex **1** (from **1.MeOH**) revealed a neutral centrosymetrical dinuclear structure in which the $(tcpd)^{2-}$ cyanocarbanion acts as a double μ_2-bridging ligand between two $[FeL]^{2+}$ (L = tmpa (**1**), andmpa (**2**)) units involving two free coordination sites in the *cis* configuration. Examination of the shortest intermolecular contacts in **1.MeOH** and **1** reveals no significant hydrogen bonding between the dinuclear units, while in **2.MeOH**, these units held together by significant hydrogen bonds between one of the uncoordinated nitrile groups and the anilate function, giving rise to 1D supramolecular structure. The three dinuclear complexes **1**, **2.MeOH** and **2** exhibit *SCO* behaviors which have been evidenced by the thermal evolutions of the $\chi_m T$ product and by the average values of the six Fe-N distances for **1** and **2.MeOH**, that reveal a gradual conversion with transition temperatures ($T_{1/2}$) at ca. 352 K (**1**), 196 K (**2**) and 180 K (2.MeOH). For the solvated **1.MeOH**, the sharp *SCO* transition observed around 365 K was induced by the desolvatation process above 330K during the magnetic measurements.

INTRODUCTION

Among the molecular switchable materials, the spin crossover (*SCO*) complexes are by far the most studied during the last decade, because of their several potential applications such as in memory display devices and sensing technology.[1-3] These complexes can be switched reversibly from a high spin (*HS*) to a low spin (*LS*) state by external stimuli such as temperature, pressure, magnetic field or light irradiation. Although the spin transition can occur in d^4-d^7 transition metal complexes, the most studied examples to date are those based on Fe(II) (d^6 configuration) metal ion, for which a paramagnetic-diamagnetic transition from *HS* (S =2) to *LS* (S = 0) is observed.[3,4] The [FeN_6] *SCO* compounds can be roughly divided into two categories: the cationic complexes in which the six donating nitrogen atoms arise from one or several neutral ligands to generate the $[FeL_n]^{2+}$ complexes, and neutral or anionic complexes for which three or four nitrogen atoms arise from neutral ligands and the octahedral environment of the iron centers completed by two or three nitrogen atoms arising from monodentate or bridging anionic ligands.[3-5] This last category which can be formulated as $[FeL_nA_m]^{0/-}$ (L = polydentate neutral ligand, A^- or A^{2-} = terminal or bridging N-donating anion) presents a richer chemical diversity since the molecular structure of the complex can be designed with a planned dimension or with a desired nuclearity, with only appropriate choice of the anionic ligand, owing to its chemical structure including its coordination properties.

In this context, we have reported in the last few years the first *SCO* series based on cyanocarbanion ligands together with abpt chelating neutral ligand (Scheme 1).[6]

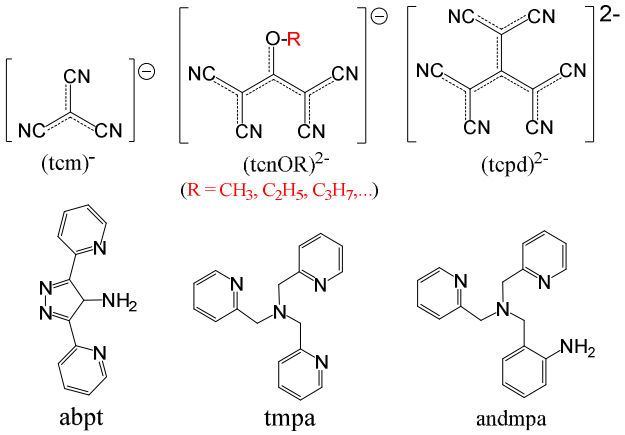

Scheme 1

In this series, the single charge on the anion induces a terminal coordination mode for the cyanocarbanion unit, resulting in neutral discrete *SCO* complexes. Afterward, we have showed, in a second report, that the use of the $(tcpd)^{2-}$ cyanocarbanion ($(tcpd)^{2-}$ = 2-

dicyanomethylene-1,1,3,3-tetracyanopropanediide anion) ligand bearing two negative charges induces bridging coordination modes to lead to an original thermo- and photo-switchable *SCO* chain.[7] In these reports, we have shown that coordination of the cyanocarbanion in the *trans* positions is clearly imposed by the planar $[Fe(abpt)_2]^{2+}$ precursor. With the aim to better explore the potential impact of such anionic ligands on the structural features of their complexes, and then on the switching properties (transition temperatures, hysteresis width, abruptness of the transition, photo-induced effects…), we have extended this work to the use of other polydentate neutral ligands such as the tris(2-pyridylmethyl)amine (Scheme 1). In contrast to the abpt bidentate ligands, such flexible tetradentate molecules should allow free coordination sites in the *cis* positions which are more appropriate for the design of polynuclear complexes.[8-11] For the tmpa ligand (tmpa = tris(2-pyridylmethyl)amine), few *SCO* systems have been reported.[8-10] The $[Fe(tmpa)]^{2+}$ entity possesses two free coordination sites in the *cis* configuration which has been used to allow the coordination of terminal ligands as observed in the polymorphic $[Fe(tmpa)(NCS)_2]$ system,[8] or the coordination of potentially bridging ligands to design polynuclear *SCO* derivatives, such as the tetranuclear complex $[Fe(tmpa)(N(CN))_2]_4$ or the diminoquinonoid-bridged dinuclear series $[Fe_2(tmpa)_2(\mu_2\text{-}^{X}L)]^{2+}$ $^{X}L^{2-}$ = double deprotonated form of 3,6-disubstituted-2,5-dianilino-1,4-benzoquinone; X = H, Br, Cl, F) in which the authors showed that the slight chemical modifications of the anionic bridging ligand ($^{X}L^{2-}$) affect strongly the transition temperature ($T_{1/2}$).[9,10]

We report herein the use of the tetradentate chelating neutral ligands in association with a cyanocarbanion bridging co-ligand to form *SCO* dinuclear complexes. We describe the syntheses, structural characterizations, including thermal variation of the crystallographic data and magnetic properties of the solvated and desolvated Fe(II) dinuclear neutral complexes $[Fe_2(tmpa)_2(\mu_2\text{-tcpd})_2]\bullet nCH_3OH$ (**1.MeOH** and **1**) and $[Fe_2(andmpa)_2(\mu_2\text{-tcpd})_2]\bullet 2CH_3OH$ (**2.MeOH** and **2**) (andmpa = (bis-(2-pyridylmethyl)aminomethyl)aniline) involving the $(tcpd)^{2-}$ anionic bridges. It should be pointed out that several *SCO* systems exhibiting dinuclear structure have been reported. Most of them, are involve neutral bridging ligands such as 2,2'-bpyrimidine,[11] 4,7-phenanthroline-5,6-diamine[12] or substituted triazole, pyrazole and thiadiazole ligands.[13] To the best of our knowledge, only one *SCO* dinuclear complex involving bridging anions has been reported.[14] Thus, the present work show that the use of cyanocarbanion ligands does not lead only to the design of polynuclear discrete complexes based on anionic bridges, but also allows the development of new neutral systems without any counter-ions.

■ RESULTS AND DISCUSSIONS.

Synthesis. The andmpa ligand was synthesized according to a two-step method described by S. Lippard,[15] which was slightly modified. The starting reactant 2-nitrobenzyl bromide was obtained as previously published, by reacting the 2-nitrobenzyl alcohol and PBr_3 in Et_2O as the solvent in place of CCl_4 (See Figure S1).[16] Reaction of this bromo- derivative with dipicolylamine (dpa) in SN2 conditions gave rise to the formation of the 2-[bis(2-pyridylmethyl)aminomethyl]nitrobenzene intermediate in 67 % yield after purification (See Figures S2 to S4). Reduction of the nitro- group into a primary amine function was carried out using hydrazine hydrate in ethanol with activated charcoal[17] instead of hydrogenation in Pd/C catalytic conditions[15] and yielded the andmpa ligand (See Figures S5 to S7) with 60 % overall yield (Scheme 2).

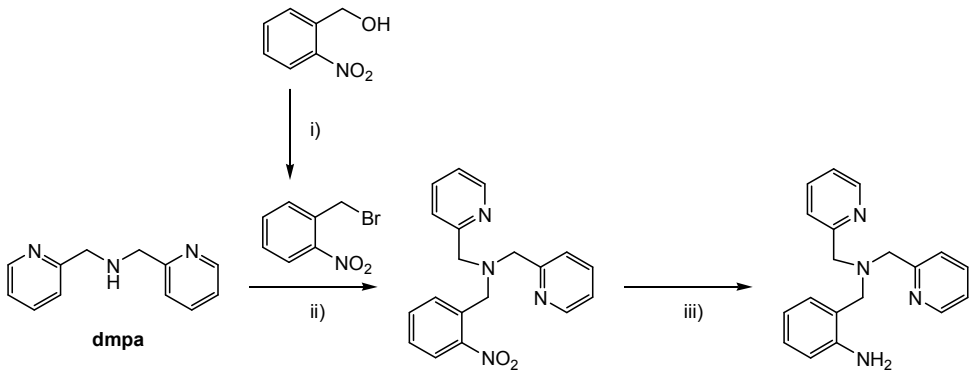

Scheme 2. Synthesis of the ligand andmpa i) 1.1 eq PBr_3, Et_2O, 0°C, 2h ; ii) K_2CO_3, CH_3CN, reflux, 5 days (67 %); iii) NH_2NH_2-H_2O, EtOH, activated charcoal, 48h (92 %).

Both Fe(II) complexes (**1.MeOH** and **2.MeOH**) were synthesized, as single crystals, using diffusion technique in fine glass tube (3.0 mm diameter) by carefully layering 2 mL of methanolic solution of K_2tcpd onto a methanolic solution containing $Fe(BF_4)_2.6H_2O$ and the tetradentate neutral ligand in 1:1 ratio (tmpa for **1.MeOH**; andmpa for **2.MeOH**). In each case, single crystals suitable for X-ray analysis were formed after three days. The single crystals of the unsolvated phase **1** $[Fe_2(tmpa)_2(\mu_2\text{-tcpd})_2]$ can be obtained either by heating the sample at 70 °C for three hours or with time at room temperature since they lose easily their solvent molecules. This "natural" desolvatation process is confirmed by single crystal X-ray diffraction at room temperature at different times and by elemental analysis since the freshly prepared single crystals of **1.MeOH** reveal only a fraction of ca. 0.3 CH_3OH (see experimental section).[18] In contrast, the two MeOH molecules in compound **2.MeOH** are clearly maintained in the crystal packing, even after their long exposition at room

temperature, as revealed by the crystal structure at 296 K. Crystals of **2.MeOH** were heated up to try to solve the crystal structure of the desolvated compound **2.** At 330 K the crystal structure reveals no significant difference with the room temperature one and confirms the presence of the two solvent molecules. Above 350 K the diffraction pattern of **2** changes drastically, highlighting the crystal damage that may be caused by the lost of the solvent molecules. Nevertheless, attempts to solve the crystal structure of **2** failed. This suggests that the solvent molecule should be involved with more and/or shorter intermolecular contacts in the crystal packing of **2.MeOH** (see below). TGA measurements performed on a set of single crystals of **2.MeOH** shows a lost of a fraction of ca. 0.27 MeOH (0.7%) at 100 °C (Figure S8). Above this temperature, additional mass loss of ca. 2.0 % has been observed, but according to the infrared spectrum of the sample maintained at 100°C during 6 hours (see experimental section) this mass loss cannot be attributed to only MeOH molecules (see below). This implies that **2.MeOH** may loss the major part of the MeOH molecules (ca. 1.73 molecules) during the preliminary vacuum procedure before the TGA experiment. Compounds **1.MeOH, 1**, **2.MeOH** and **2** display similar infrared patterns (See Figures S9 and S10). The infrared spectrum of **2.MeOH** displays a broad absorption bands around 3468 cm^{-1}. This band which was not observed on the infrared spectra of the warmed samples (see Figure S10), can be attributed to OH stretching of the MeOH molecules in **2.MeOH**. As expected, the four complexes (**1.MeOH, 1**, **2.MeOH** and **2**) show absorption bands assigned to the ν_{CN} stretching vibrations of the cyanocarbanion (2192 and 2165 cm^{-1} for **1.MeOH**; 2192 and 2166 cm^{-1} for **1**; 2186 and 2161 cm^{-1} for **2.MeOH**; 2187 and 2165 cm^{-1} for **2**). These absorption bands, distinct from the stretching vibration modes observed for the tetrabutylammonium salt ($[(C_4H_9)_4N]_2$(tcpd)) containing the uncoordinated cyanocarbanion units (2094-2174 cm^{-1}),[7] can be assigned to the presence of both bridging (2192-2186 cm^{-1}) and terminal (2161-2166 cm^{-1}) nitrile groups, in agreement with the single crystal structure determination (see below).

Description of the Crystal structures. Pertinent crystal data and selected bond distances and bond angles for compounds **1.MeOH**, **1** and **2.MeOH** are summarized in Tables 1-4 and S2. The molecular structures are depicted in Figures 1-2. The three compounds crystallize in the monoclinic $P2_1/n$ space group for all the studied temperatures (Table 1 and Table S1).

Table 1. Crystal data and structural refinement parameters for compounds **1.MeOH, 1** and **2.MeOH**

	1.MeOH	**1**		**2.MeOH**	
Temperature / K	296(2)	296(2)	380(2)	100(2)	296(2)
[a]Empirical formula	$(C_{56}H_{36}Fe_2N_{20})$, $0.8(CH_3OH)$	$C_{56}H_{36}Fe_2N_{20}$		$(C_{58}H_{40}Fe_2N_{20})$, $2(CH_3OH)$	
Formula weight /g.mol^{-1}	1127.49	1100.75		1192.88	
Wavelength / Å	0.71073 Å	0.71073 Å		0.71073 Å	
Crystal system	Monoclinic	Monoclinic		Monoclinic	
Space group	$P2_1/n$	$P2_1/n$		$P2_1/n$	
a / Å	11.7269(5)	11.468(4)	10.894(4)	9.6690(10)	9.6831(12)
b / Å	16.6966(6)	17.0057(9)	18.7523(9)	24.658(2)	25.065(3)
c / Å	13.9317(6)	13.7743(6)	13.7750(6)	11.5670(10)	12.0485(16)
β /°	104.672(4)	105.098(9)	106.492(9)	102.631(6)	103.711(14)
Volume / Å^3	2638.87(19)	2593.6(10)	2698.3(11)	2691.0(4)	2840.9(7)
Z	2	2	2	2	2
D_{calc} / g.cm^{-3}	1.419	1.409	1.355	1.472	1.395
CCDC No.	1413422	1435809	1435810	1413424	1413423

[a]The asymmetric unit contains 0.5 of the chemical formula.

The asymmetric unit of **1.MeOH** is built from one Fe(II) ion, one tmpa neutral ligand, one $(tcpd)^{2-}$ anion and a methanol solvent molecule with a partial occupation factor of 0.4 at room temperature, all located on general positions. The molecular structure of **1.MeOH** consists of centrosymmetric neutral dinuclear entities of the formula $[Fe_2(tmpa)_2(\mu_2\text{-}tcpd)_2]$ and 0.8 methanol molecule (Figure 1).

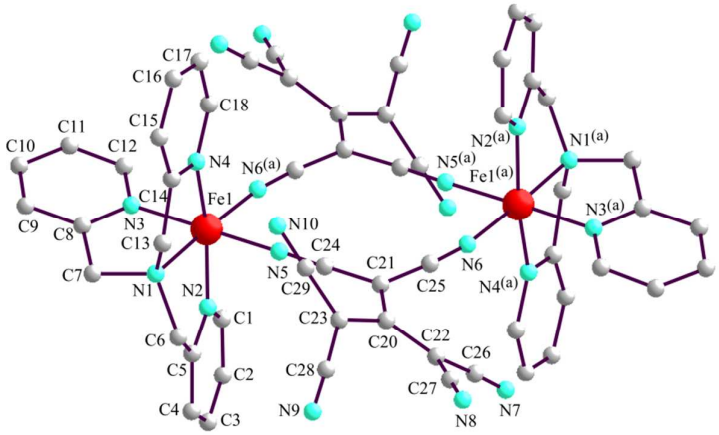

Figure 1. Molecular structure of the dinuclear iron (II) complex of **1,** (a) = 1-x,-y,-z+2.

Except the absence of MeOH solvent molecules, the asymmetric unit of **1** is similar to that observed for compound **1.MeOH**, and the two complexes are isostructural with only slight structural differences. In both complexes, the tmpa molecule acts as a tetradentate ligand leading to the $[Fe(tmpa)]^{2+}$ entities which are connected by two $(tcpd)^{2-}$ anions acting as μ_2–bridging ligands through two nitrile groups of the same $C(CN)_2$ wing. Each iron (II) metal ion presents a distorted FeN_6 octahedral environment assumed by four nitrogen atoms (N1, N2, N3, N4) arising from the tmpa ligand and by two nitrogen atoms of two equivalent $(tcpd)^{2-}$ anions (N5 and $N6^{(a)}$).

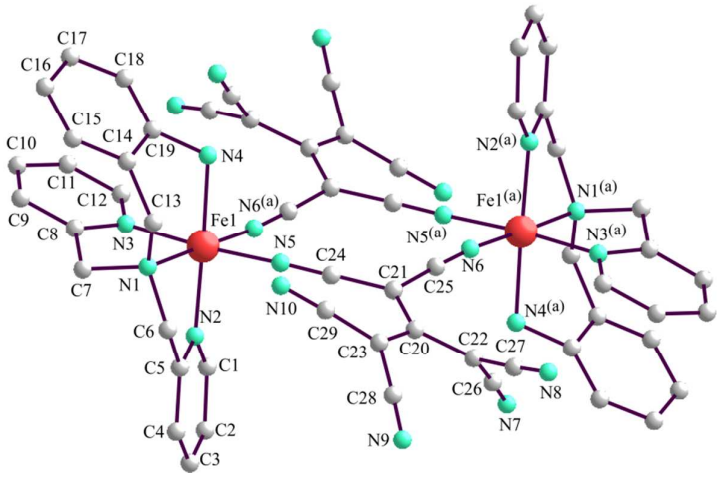

Figure 2. Molecular structure of the dinuclear iron (II) complex of **2,** (a) = -x,-y+1,-z+1

For compound **2.MeOH**, the crystallographic parameters are different from those observed for compounds **1.MeOH** and **1** (see Table 1). Despite this difference, the structure of **2.MeOH** is built from similar asymmetrical unit, leading to a dinuclear molecular structure of the formula $[Fe_2(andmpa)_2(\mu_2\text{-}tcpd)_2]\bullet 2CH_3OH$, similar to that described for **1.MeOH** (Figure 2). Examination of the shortest intermolecular contacts in **1.MeOH** and **1** reveals no significant hydrogen bonding between the dinuclear units, excepting the hydrogen bonding observed between the dinuclear units and the oxygen of the methanol molecule (Table 3, Figure 3a) in **1.MeOH**. However, as depicted in Figure 3a, the packing cohesion in **1.MeOH** and **1** is ensured by the π-π like contacts between the π-delocalized parts of the tcpd anions of the adjacent dinuclear units (see Table 2b). Additionally to the hydrogen bond mentioned above, the MeOH molecule is also stabilized by several Van der Waals interactions involving the carbon atoms of the tcpd anion and the tmpa ligand (Table 2a). Despite the loss of the solvent molecule, the packing cohesion in **1** is very similar to that in **1.MeOH** but with slightly more pronounced π-π contact between the tcpd anions (Table 2b). In contrast, a different situation is observed in complex **2.MeOH** since the dinuclear units held together by

significant hydrogen bond between the anilate -NH_2 group (N4) of the andpma ligand and one of the uncoordinated nitrile groups (N4…N8: 3.183(6) Å), giving rise to 1D supramolecular structure as highlighted in Figure 3b. As in **1**, the adjacent $(tcpd)^{2-}$ anions are involved in π-π like contacts between π-delocalized parts of tcpd anions and hydrogen bonding (O1…N9: 2.843(7) Å) occurs between the methanol molecule (O1) and one of the non coordinated nitrile groups (N9) of the cyanocarbanion (see Tables 2-3).

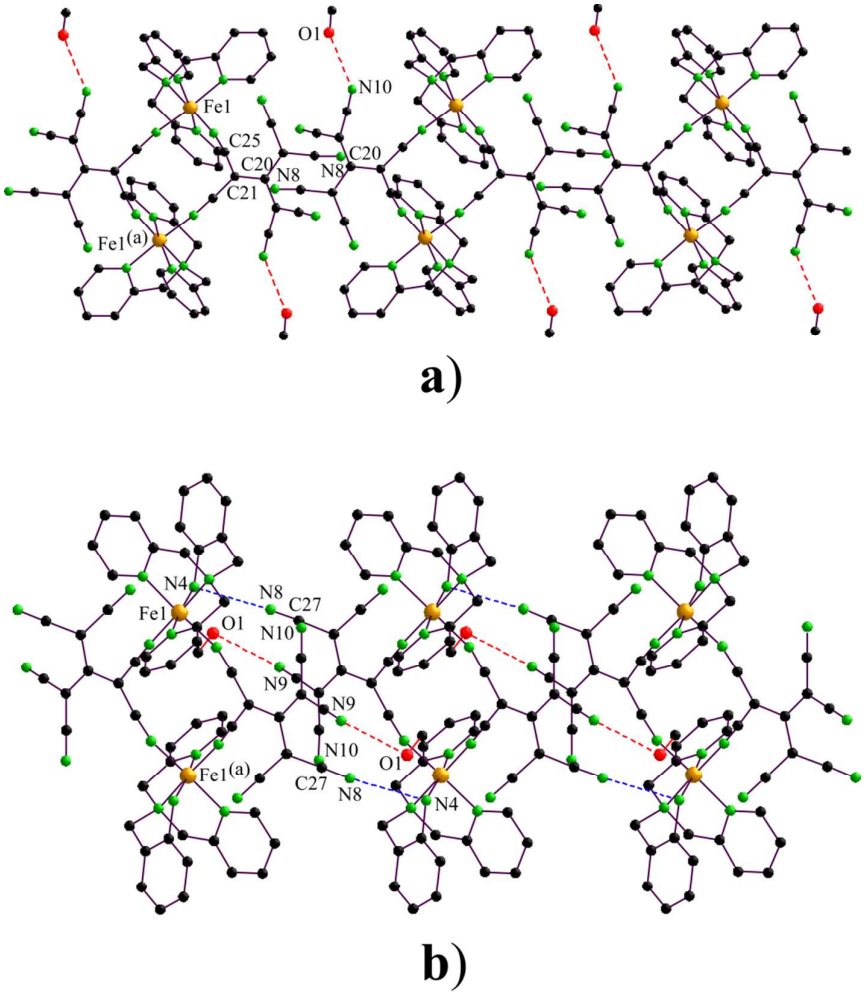

Figure 3. Intermolecular contacts in compounds **1.MeOH** (**a**) and **2.MeOH** (**b**).

According to Table 3, this hydrogen bond is slightly stronger in **2.MeOH** than in **1.MeOH** as O-H···N angle is more linear in **2.MeOH.** It is worth to note that the MeOH molecule is also involved in Van der Waals interactions that are more numerous in **2.MeOH** than in **1. MeOH.** Both observations are consistent with the fact that the MeOH molecules remain in the network of **2.MeOH** at room temperature whereas they slowly go out the crystal of **1.MeOH** as revealed by variable temperature X-ray data collections and also by the elemental analysis.

Table 2a. Shortest intermolecular contacts (Å) in **1.MeOH**, **1** and **2.MeOH** at 296 K

	1.MeOH	**1**	**2.MeOH**
(tcpd)N8···C20[(a)](tcpd)	3.327(5)	3.359(4)	
(tcpd)N8···C21[(a)](tcpd)	3.328(4)	3.278(4)	
(tcpd)N8···C25[(a)](tcpd)	3.362(4)	3.294(4)	
(tcpd)N10···C27[(b)](tcpd)			3.388(8)
(tcpd)C25···C29[(b)](tcpd)			3.590(7)
(an)N4···N8[(b)](tcpd)			3.183(6)
(MeOH)O1···N10[(c)](tcpd)	2.849(8)		
(MeOH)O1···C6[(b)](am.Me)	3.273(9)		
(MeOH)C30···C20(tcpd)	3.388(10)		
(MeOH)C30···C22(tcpd)	3.5366(11)		
(MeOH)C30···C11[(d)](py)	3.558(12)		
(MeOH)O1···C4[(b)](py)	3.169(9)		
(MeOH)O1···C4[(e)](py)			3.265(8)
(MeOH)O1···C10[(f)](py)			3.258(7)
(MeOH)C30···N9[(b)](tcpd)			3.346(9)
(MeOH)C30···C24[(g)](tcpd)			3.557(9)
(MeOH)C30···C25[(g)](tcpd)			3.566(9)
(MeOH)C30···C21[(g)](tcpd)			3.580(9)
(MeOH)C30···C1[(g)](py)			3.581(9)
(MeOH)O1···N9[(b)](tcpd)			2.843(7)

(a) = 2-x, 1-y, 2-z; (b) = 1-x,1-y,1-z ; (c) = 3/2-x, y-1/2, 3/2-z; (d) = 1/2-x, y-1/2, 3/2-z; (e) = x, y, 1+z; (f) = 1/2+x, 3/2-y, 1/2+z; (e) = -x, 1-y,1-z; (tcpd) = the involved atom belongs to the tcpd anion; (an.) the involved atom belongs to the anilate moiety; (am.Me) the involved atom belongs to the amino-methyl moiety; (py) the involved atom belongs to the pyridin moiety; (MeOH) the involved atom belongs to the methanol molecule.

Table 2b. π-π like intermolecular contacts (Å) in **1**, **1.MeOH** and **2.MeOH** at 296 K

compound	π system[(1)]	c-c[(2)] / Å	Shift[(3)] / Å	Angle[(4)] / °
1	C20C21C22C23C27N8[(a)]	3.605(2)	1.088(4)	0.00(2)
1.MeOH	C20C21C22C23C27N8[(a)]	3.658(2)	1.303(4)	0.0(3)
2.MeOH	C20C21C22C23C29N10[(b)]	3.672(4)	0.488(8)	0.00(3)

(1) The intermolecular interaction involves the defined π system and its symmetry equivalent at (a) = 2-x, 1-y, 2-z and (b) =1-x, 1-y, 1-z. (2) centroid to centroid distance. (3) shift distance (4) Angle between planes.

Table 3. Hydrogen bonds in **1.MeOH** and **2.MeOH** at 296 K.

compound	D-H···A	**d(D-A)/Å**	**d(D-H···A)/Å**	**D-H-A/°**
1.MeOH	**(MeOH)**O1-H···N10[(a)](tcpd)	2.849(8)	2.079(3)	156.4(8)
2.MeOH	**(MeOH)**O1-H···N9[(b)](tcpd)	2.843(7)	2.045(5)	164.7(4)
2.MeOH	(an.)N4-H4b···N8[(b)](tcpd)	3.183(6)	2.215(5)	175.1(3)

(a) = 3/2-x, y-1/2, 3/2-z; (b) = 1-x,1-y,1-z ; (tcpd) = the involved atom belongs to the tcpd anion ; (an.) the involved atom belongs to the anilate moiety ; (MeOH) the involved atom belongs to the methanol molecule.

Magnetic Properties. The thermal dependence of the product of the molar magnetic susceptibility times the temperature ($\chi_m T$) for this dinuclear family has been studied on single crystal samples in the temperature range 10-395 K. Concerning compound **1.MeOH**, it has been inserted at 150 K in the SQUID magnetometer to prevent easy solvent loss. The temperature then has been increased up to 395 K (Figure 4). From 150 K to 275 K, the $\chi_m T$ value remains close to zero (0.12 cm^3 K mol^{-1}), in agreement with a low spin state of the Fe(II) ions. From 275 K to 330 K, a slight increase of $\chi_m T$ is observed followed by a sharp increase above 330 K. At 395 K, the $\chi_m T$ value of 5.95 cm^3 K mol^{-1} is reached, which is slightly lower than that the expected value for two Fe(II) HS (between 6 and 7 cm^3 K mol^{-1} depending on the g value). This behavior is relevant with a desolvation occurring above 330 K, inducing a spin-crossover. The curve's shape indicates that even at 395 K, this spin-crossover is not complete and that a small amount of Fe(II) should stay in the LS state. Upon cooling, a new curve is described that present a gradual decrease of the $\chi_m T$ value down to 0.37 cm^3 K mol^{-1} at 150K, without any clear steps. This curve appears stable upon further temperature cycling (Figure S11). Regarding the ability of **1.MeOH** to lose its solvent, this second *SCO* complex, characterized by a $T_{1/2}$ of 352 K, could be assigned to compound **1**.

Compound **2.MeOH** shows a room temperature $\chi_m T$ value of 6.29 $cm^3 \cdot K \cdot mol^{-1}$, in agreement with the presence of two isolated *HS* Fe(II) metal ions with a *g* value of 2.05. The $\chi_m T$ product for **2.MeOH** smoothly decreases upon cooling down to 0.21 $cm^3 \cdot K \cdot mol^{-1}$ at 50 K (Figure 4). This *HS*↔*LS SCO* conversion is characterized by a $T_{1/2}$ value of 180 K and is reversible upon warming and cooling (Figure S12). After warming at 350 K for half an hour, the thermal behavior of the sample was recorded. A slightly more abrupt curve is observed (Figure 4) that could be related to the spin-crossover of the desolvated compound **2**, with a $T_{1/2}$ value of 196 K. This spin-crossover curve is reversible upon cooling and warming (Figure S13).

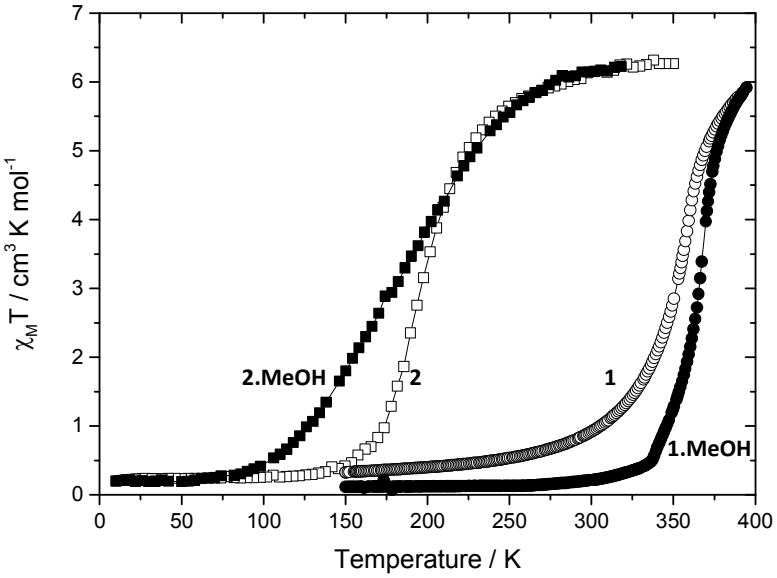

Figure 4. Thermal variation of the $\chi_m T$ product of **1.MeOH** (●), **1** (o), **2.MeOH** (■) and **2** (□), measured at 1 K/mn in settle mode for **2.MeOH** and **2** and in sweep mode in **1.MeOH** and **1**.

The solvent dependent magnetic behavior is commonly reported in the *SCO* literature. In the binuclear case this is less common. Indeed, apart from the report of new binuclear units, few examples are related to the influence of counter-anion and solvent.[13a-b,14,19] The amount and nature of solvent could strongly affect the magnetic properties, affecting the presence of multi-step spin-crossover behavior. Among the more than 30 binuclear systems reported both one and two-step spin crossover behaviors are described.[20] Up to now there is no clear understanding of the occurrence or not of steps along the transition. The main theoretical approach evidenced that stepped transition could follow from elastic strains within the molecules and/or the network.[21] However, from the structural point of view this is not always obvious and this point would deserve more attention.[22]

Magneto-structural relationships. Based on the conclusions derived from the magnetic data, the crystal structures of both compounds have been determined at different temperatures (380 K for **1** and 100 K for **2.MeOH**), to know more about the two spin states of each dinuclear complex. To know how the crystal structure and the two iron (II) sites are affected by the incomplete *SCO* transition observed for **1**, the temperature dependence of its crystal structure was performed in the temperature range 296-380 K. The corresponding structural parameters are depicted in Table 4 and in Figure 5. These crystallographic data, such as unit cell volume, the average Fe-N distances ($<Fe\text{-}N>_{LS}$ ~ 2.0 Å; $<Fe\text{-}N>_{HS}$ ~ 2.2 Å) and the trigonal distortion parameters Σ and Θ (see Table 4),[23-25] are known to be highly sensitive to the spin state of the Fe(II) centers, and will thus be used to assign the spin state of Fe(II) sites in each complex.

Table 4. Selected bond lengths (Å) and distortion parameters of the coordination sphere in **1**-**2**.

	1.MeOH	**1**		**2.MeOH**	
***T* / K**	**296**	**296**	**380**	**100**	**296**
Fe1-Fe1[(a)]	7.0752(7)	7.1242(8)	7.2688(15)	7.1732(11)	7.3377(16)
Fe1-N1	1.985(2)	1.991(2)	2.191(4)	2.025(3)	2.232(4)
Fe1-N2	1.973(2)	1.973(2)	2.131(6)	1.973(3)	2.145(4)
Fe1-N3	1.966(2)	1.971(2)	2.149(5)	1.972(3)	2.136(4)
Fe1-N4	1.975(2)	1.973(2)	2.121(5)	2.068(3)	2.200(4)
Fe1-N5	1.949(3)	1.951(3)	2.118(6)	1.956(3)	2.149(4)
Fe1-N6[(a)]	1.939(3)	1.939(2)	2.055(5)	1.955(3)	2.100(4)
<Fe-N>	**1.965(3)**	**1.966(3)**	**2.128(5)**	**1.992(3)**	**2.160(4)**
Distorsion					
[b]Σ(Fe1) (°)	51(2)	56(2)	94(3)	48(2)	75(2)
[c]Θ(Fe1) (°)	133(3)	143(3)	248(5)	141(4)	214(4)

(a) = 1-x,-y,-z+2 (**1.MeOH** or **1**) or -x,-y+1,-z+1 (**2.MeOH**)
[b]Σ is the sum of the deviation from 90° of the 12 *cis*-angles of the FeN_6 octahedron;[23-24] [c]Θ is the sum of the deviation from 60° of the 24 trigonal angles of the projection of the FeN_6 octahedron onto its trigonal faces.[24-25]

The iron centers present an octahedral FeN_6 geometry for all compounds. In good agreement with the magnetic data, the mean Fe-N distances observed at 296 K for the solvated (**1.MeOH**) and for the unsolvated phase (**1**) (1.965(3) and 1.966(3) Å, respectively) are in the range of those expected for Fe(II) ion in the *LS* state,[6,7] The octahedral geometry appears slightly more distorted for compound **1** than for **1.MeOH** since the trigonal distortion parameter calculated for **1** (Θ = 143(3)°) is higher than the corresponding value calculated for **1.MeOH** (Θ = 133(3)°). At 380 K, **1.MeOH** irreversibly loses its methanol molecule

becoming **1**. The coordination sphere volume of the metal increases as the mean Fe-N distance rises to 2.128(5) Å and conjointly the octahedral geometry becomes more distorted (see Tables 4 and S2), suggesting a *LS*→*HS* transition. Nevertheless, the mean Fe-N distance (2.128(5) Å) appears significantly smaller than that observed for the *HS* Fe(II) in compound **2.MeOH** (2.160(4) Å) at 296 K) and smaller than those generally observed for other Fe(II) compounds. This can be due to an incomplete spin transition at 380 K for **1**, corresponding to a small amount of remaining *LS* Fe(II) in the crystal structure. Even if this observation agrees perfectly the magnetic observations, the crystal data at 380 K did not reveals clearly if at this temperature, the plateau corresponding to the *HS* sate is reached. Thus, in order to investigate further this incomplete spin transition, the crystal structure of compound **1** has been solved every 5 K between 296 K and 380 K (see Table 1 for 296 and 380 K; and CCDC numbers 1442955-1442970 for the temperature range 300-375 K). These additional structural investigations did not reveal any lost of symmetry on the whole temperature range suggesting that both iron centers of the dinuclear complex are similarly affected by the spin transition, which is consistent with the observed one-step transition from [LS-LS] to [HS-HS] states. According to Figure 5, that shows the evolution of the unit cell volume and the mean Fe-N bond length between 296 K and 380 K, the incomplete spin transition reaches a plateau at 370 K, revealing that the fraction of about 20 % of the complex is trapped in the *LS* state.

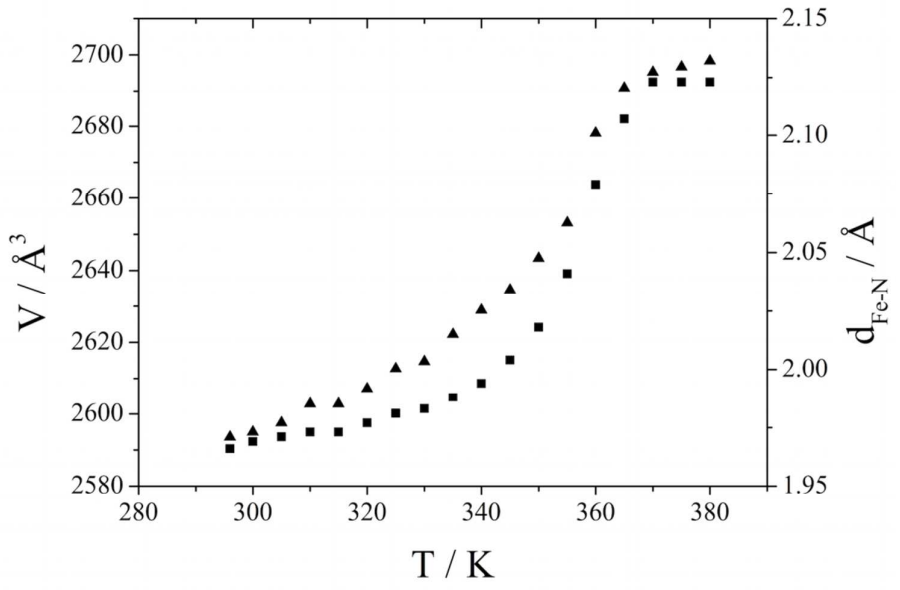

Figure 5. Evolution of the unit cell volume (▲) and the mean Fe-N distance (■) for compound **1** from room temperature to 380 K.

For compound **2.MeOH**, the mean Fe-N distance observed at room temperature (d_{Fe-N} = 2.160(4) Å) is characteristic of the presence of the iron (II) ion in the *HS* state. At 100 K, the octahedral geometry of **2.MeOH** becomes more regular and the mean Fe-N distance decreases drastically to reach 1.992(3) Å. In agreement with the magnetic data, this feature is the signature of the change of the spin state from *HS* to *LS* at low temperature.

■ CONCLUSIONS

Four dinuclear complexes of formula $[Fe_2(L)_2(\mu_2\text{-tcpd})_2]\bullet nCH_3OH$ are obtained from reaction of two tetradentate neutral ligands (L = tmpa (**1.MeOH** and **1**) and L = andmpa (**2.MeOH** and **2**)) and the bridging $(tcpd)^{2-}$ anionic ligand. The complexes display similar molecular structures described as neutral dinuclear units involving similar double μ_2-tcpd bridges. However, as shown by their crystallographic parameters and confirmed by the intermolecular contacts, the tmpa (**1.MeOH** and **1**) and the andmpa (**2.MeOH**) complexes display different crystal packing. One of the principle objectives of this study concerns the investigation of the subtle chemical substitution of the tetradentate ligand on the *SCO* behavior. Complex **1.MeOH** based on the tmpa ligand shows *LS* state even at room temperature but undergoes an incomplete spin crossover around 365 K which was probably induced by the desolvatation of the sample above 330 K. The crystallographic structural studies confirm clearly the total desolvatation of **1.MeOH** at 380 K, leading to compound **1** without drastic structural changes. This desolvated complex (**1**) reveals a slightly more gradual *SCO* behavior at ca. 352 K. Complex **2.MeOH** involving a slightly different tetradentate ligand (andmpa) shows a *SCO* behavior with a transition temperature of *ca.* 180 K, after desolvatation a more abrupt *SCO* occurs at a slightly higher temperature ($T_{1/2}$ = 196 K). The two desolvatation process (**1.MeOH→1** and **2.MeOH→2**) show only slight modification of the *SCO* behaviors while the strong changes of the transition temperatures have been observed between compounds **1** and **2** ($\Delta(T_{1/2}) > 150$ K). Finally, It is worthy to note that this drastic evolution of the transition temeprature cannot be attributed exclusively to the ligand substitution performed on the tmpa initial ligand but also to the solid-state packing which affects significantly the elastic interactions and the *SCO* behavior as exemplified by several polymorphic systems.[8,26]

EXPERIMENTAL SECTION

General Remarks. Tetracyanoethylene, urea, potassium tert-butoxide (C_4H_9OK), malononitrile ($CH_2(CN)_2$), 2-nitrobenzyl alcohol, di-picolyl amine, PBr_3, K_2CO_3 and $Fe(BF_4)_2.6H_2O$ were purchased from commercial sources and used without further purification. Solvents were used and purified by standard procedures. The organic ligands have been prepared under nitrogen. The potassium salt K_2(tcpd) and tmpa ligand (tris(2-pyridylmethyl)amine) were prepared according to published procedures (See Figures S14 to S16).[27-28] Elemental analyses were performed by the "Service Central d'Analyses du CNRS", Gif-sur-Yvette, France. Infrared spectra were recorded in the range 4000-200 cm^{-1} on a FT-IR Brucker ATR Vertex 70 Spectrometer. Diffraction analyses were performed using an Oxford Diffraction Xcalibur κ-CCD diffractometer. NMR spectra were recorded on a Brucker DRX 300 MHz or Brucker Avance 400 and 500 MHz. TGA measurements were performed on Symmetric TGA Setaram TAG2400. The sample was preliminary put under vacuum and then heated at 3°C.min^{-1} under an Argon atmosphere. Magnetic measurements were performed with a Quantum Design MPMS-XL-5 SQUID magnetometer in the 10-400 K temperature range with an applied magnetic field of 2 T on crushed single crystals of compounds **1.MeOH** and **2.MeOH**. The susceptibility data were corrected for the sample holders previously measured under the same conditions, and for the diamagnetic contributions as deduced by using Pascal´s constant tables (χ_{dia} = -547.4x10^{-6} and -571.6x10^{-6} emu•mol^{-1} for **1.MeOH** and **2.MeOH**, respectively).[29]

Crystallographic Data Collection and Refinement. Crystallographic studies of the two derivatives (**1**-**2**) were performed at 296 K, 100 K and 380 K, using an Oxford Diffraction Xcalibur κ-CCD diffractometer equipped with a graphite monochromated Mo$K\alpha$ radiation (λ = 0.71073 Å) or a Brucker APEX-II CCD diffractometer (λ = 0.71073 Å). At 380K a crystal of 1 has been mounted on a glass fiber and glued with high temperature resisting structural glue (DP700 Epoxy structural adhesive from 3M Scotch-WeldTM) and then collected on a Brucker APEX-II CCD diffractometer (λ = 0.71073 Å). The full sphere data collections were performed using 1.0° ω-scans with an exposure time of 200 s and 35s per frame for **1.MeOH** and **1**, 60 s and 80 s per frame for **2.MeOH** at 296 K and 100 K, respectively. Data collection and data reduction were done with the CRYSALIS-CCD and CRYSALIS-RED programs or on the Brucker APEX-II program suite on the full set of data.[30] The crystal structures were solved by direct methods and successive Fourier difference syntheses, and were refined on F^2 by weighted anisotropic full-matrix least-square methods.[31]

All non-hydrogen atoms were refined anisotropically, while the hydrogen atoms were calculated and therefore included as isotropic fixed contributors to F_c. All other calculations were performed with standard procedures (WINGX, OLEX2).[32-33] Pertinent crystal data, structure refinement and collection parameters are listed in Table S1.

Synthesis of Bis-(2-pyridylmethyl)aminomethyl)aniline (**andmpa**). 2-nitrobenzylbromide (1.08g, 5.0 mmol) was added to a solution of bis(2-pyridylmethyl)amine (dmpa) (1.00 g, 5.0 mmol) in distilled CH_3CN (20mL) with K_2CO_3 (1.38 g, 10.0 mmol). The reaction mixture was heated to reflux with stirring for 5 days. After cooling and filtration of the solution, the solvent was removed by evaporation. Purification of the crude product by column chromatography on neutral alumine (CH_2Cl_2/MeOH from 100/0 to 99/1) produced a brown oil of bis-(2-pyridylmethyl)aminomethyl)nitrobenzene (1.12 g, 67 %). IR data (ν/cm^{-1}): 3060(w), 3008(w), 1588(m), 1569(m), 1523(s), 1432(m), 1358(m), 764(m), 731(m); ^{1}H NMR δ (300MHz, $CDCl_3$) 3.78 (4H, s, CH_2), 4.07 (2H, s, CH_2), 7.12 (2H, dd), 7.33 (1H, t), 7.40 (2H, d), 7.48 (1H, t), 7.63 (2H, t), 7.70 (1H, d), 7.75 (1H, d), 8.49 (d, 2H) ^{13}C NMR δ (75MHz, $CDCl_3$): 55.7 60.3(2C) (*C*H_2); 121.9(2C), 123.1(2C), 124.2 127.8 131.2 132.2(C_{quat}), 134.2(2C), 148.8(2C), 149.8($_{Cquat}$), 158.5(C_{quat}) ($C_{aromatic}$). Oxygen-free hydrazine hydrate (15 mL, excess) (***Caution.*** *Harmful and unstable, should be used carefully!*) was added to a solution of bis-(2-pyridylmethyl)aminomethyl)nitrobenzene (1.00 g, 3.0 mmol) in absolute ethanol (50 mL) with activated carbon (1.0 g). The reaction mixture was heated to reflux with stirring under nitrogen atmosphere for 48 hours. After cooling, the solution was filtered through celite and the filtrate was evaporated under reduced pressure. The residue was dissolved in $CHCl_3$ (30 mL) and dried with $MgSO_4$. After filtration, the solvent was removed to yield a brown solid of bis-(2-pyridylmethyl)aminomethyl)aniline (andmpa) (840 mg, 92 %). IR data (ν/cm^{-1}): 3401(m), 3312(m), 3201(m), 1633(m), 1589(s), 1492(m), 1432(m), 752(vs); ^{1}H NMR δ (300MHz, $CDCl_3$) 3.66 (2H, s, CH_2), 3.79 (2H, s, CH_2), 6.61-6.64 (2H, m), 7.02-7.05 (2H, m), 7.11-7.15 (m, 2H), 7.36 (d, 2H), 7.62 (t, 2H), 8.53 (d, 2H); ^{13}C NMR δ (75MHz, $CDCl_3$) 57.6 59.9(2C) (CH_2), 115.2 116.9 121.8(2C) 122.0(C_{quat}), 123.2(2C), 128.2 130.9 136.1(2C), 146.8(C_{quat}), 148.8(2C), 158.9(C_{quat}) ($C_{aromatic}$).

Complex Syntheses. $[Fe_2(tmpa)_2(\mu_2\text{-tcpd})_2]\bullet nCH_3OH$ (**1.MeOH**)**:** $Fe(BF_4)_2.6H_2O$ (6.7 mg, 0.02 mmol) was added to a solution of tmpa (0.02 mmol, 5.8 mg) in methanol (2mL). The resulting yellow solution was placed in a glass capillary (diameter 0.3 mm). Then a solution of K_2tcpd (5.6 mg, 0.02 mmol) in methanol (2 mL) was carefully added in the capillary. Red crystals suitable for X-ray diffraction were obtained after 3 days (yield: 5.0 mg, 44.5 %).

Anal. Calcd. (%) for $[C_{56}H_{36}Fe_2N_{20}](CH_3OH)_n$ for n = 0.3 C, 60.9; H, 3.4; N, 25.2. Found (%): C, 61.3; H, 3.4; N, 25.4. IR data (ν/cm^{-1}): for the freshly filtered sample: 3417(br), 3079(w), 2192(s), 2165(s), 1606(m), 1433(s), 1399(s), 1287(w), 1243(m), 1157(w), 1034(w), 991(m), 759(s),735(m), 644(w), 503(w, 466(m), 443(m). The unsolvated phase of **1.MeOH** $[Fe_2(tmpa)_2(\mu_2\text{-tcpd})_2]$ (**1**) has been prepared easily by heating the sample at 70 °C during three hours. Anal. Calcd. (%) for $[C_{56}H_{36}Fe_2N_{20}]$: C, 61.1; H, 3.3; N, 25.5. Found (%): C, 61.5; H, 3.3; N, 25.8.[18] IR data (ν/cm^{-1}): 3073(w), 2925(w), 2192(s), 2166(s), 1606(m), 1481(m), 1433(s), 1400(s), 1304(w),1288(w), 1244(m), 1156(w), 1097(s), 1055(w), 1025(w), 991(m), 761(s), 735(m), 686(w), 644(w), 541(w), 502(w), 467(m), 442(m), 406(m). $[Fe_2(andmpa)_2(\mu_2\text{-tcpd})_2]\bullet 2CH_3OH$ (**2.MeOH**): $Fe(BF_4)_2.6H_2O$ (6.7 mg, 0.02 mmol) was added to a solution of andmpa (0.02 mmol, 6.1 mg) in methanol (2 mL). The resulting yellow solution became green after standing overnight, and then placed in a glass capillary (diameter 0.3 mm). A solution of K_2tcpd (5.6 mg, 0.02 mmol) in methanol (2 mL) was carefully added in the capillary. Green crystals suitable for X-ray diffraction were obtained after 3 days (yield: 4.2 mg, 35.5 %). Anal. Calcd. (%) for $C_{60}H_{48}Fe_2N_{20}O_2$: C, 60.4; H, 4.1; N, 23.5. Found (%): C, 59.9; H, 4.2; N, 23.2. IR data (ν/cm^{-1}): 3468(m); 3268(w), 3213(w), 3134(w), 2922(w), 2854(w), 2186(s), 2161(s), 1442(s), 1390(s), 1294(w), 1241(w), 1035(s), 1020(s), 867(m), 762(s), 736(m), 688(m), 642(w), 619 (w), 572(w), 539(m), 509(s), 488(w), 476(w) 424(w). The unsolvated phase of **2.MeOH** $[Fe_2(andmpa)_2(\mu_2\text{-tcpd})_2]$ (**2**) has been prepared by heating the sample at 100 °C during 6 hours. Anal. Calcd. (%) for $[C_{58}H_{40}Fe_2N_{20}]$: C, 61.7; H, 3.5; N, 24.8. Found (%): C, 62.1; H, 3.7; N, 24.3. IR data (ν/cm^{-1}): 3221(w), 3129(w), 2922(w), 2857(w), 2187(s), 2165(s), 1606(m), 1436(s), 1387(s), 1295(w), 1151(w), 1081(m), 1020(m), 867(m), 759(s), 737(m), 688(w), 643(w), 539(m), 508(m), 488(w), 419(w).

■ ASSOCIATED CONTENT

Supporting information

The Supporting Information is available free of charge on the ACS Publications website at DOI: XXXXX/acs.inorg-chem.XXXXXXX

X-ray crystallographic data in CIF format: CCDC numbers 1413422 (**1.MeOH** at 296 K), 1413423–1413424 (**2.MeOH** at 296 and 100 K, respectively), 1435809-1435810 (**1** at 296 and 380 K, respectively) and 1442955-1442970 (**1** from 300 to 375 K, respectively) (CIF).

■ AUTHOR INFORMATION

Corresponding author

*E-mail: smail.triki@univ-brest.fr

Author Contributions

The manuscript was written through contributions of all authors.

Notes

The authors declare no competing financial interest.

■ ACKNOWLEDGMENTS

This work is supported by the CNRS (Centre National de la Recherche Scientifique), the Brest University, the "Agence Nationale de la Recherche" (ANR project BISTA-MAT: ANR-12-BS07-0030-01), the Aquitaine Region for the support of the International Center of Photomagnetisme in Aquitaine. Authors especially thank the “Service Commun” of NMR facilities of the University of Brest and D. Denux from thermic measurements of ICMCB for the TGA analysis.

■ REFERENCES

(1) see for example: a) Gómez, V.; Sáenz de Pipaón, C.; Maldonado-Illescas, P.; Waerenborgh, J.-C.; Martin, E.; Benet-Buchholz, J.; Galán-Mascarós, J.-R., *J. Am. Chem. Soc.* **2015**, *137*, 11924–11927; b) Chen, M.-Y.; Chen, X.-R.; Ninga, W.-H.; Ren, X.-M., *RSC Adv.* **2014**, *4*, 39126–39131; c) Kahn, O.; Martinez, C. J., *Science* **1998**, *279*, 44–48; d) Bousseksou, A.; Molnár, G.; Demont, P.; Menegotto, J., *J. Mater. Chem.* **2003**, *13*, 2069-2071; e) Dugay, J.; Giménez-Marqués, M.; Kozlova, T.; Zandbergen, H. W.; Coronado, E.; van der Zant, H. S. J., *Adv. Mat.* **2015**, 27, 1288-1293.

(2) a) Bartual-Murgui, C.; Akou, A.; Thibault, C.; Molnár, G.; Vieu, C.; Salmon, L.; Bousseksou, A., *J. Mater. Chem. C*, **2015**, *3*, 1277-1285; b) Jureschi, C. M.; Rusu, I.; Codjovi, E.; Linares, J.; Garcia, Y.; Rotaru, A., *Physica B* **2014**, *449*, 47–51; c) Linares, J.; Codjovi, E.; Garcia, Y., *Sensors* **2012**, *12*, 4479–4492; d) Real, J. A.; Gaspar A. B.; Niel, V.; Muñoz, M.-C., *Coord. Chem. Rev.* **2003**, *236*, 121-141.

(3) a) Sertphon, D.; Harding, D. J.; Harding, P.; Murray, K. S.; Moubaraki, B.; Adams, H.; Alkas, A.; Telfer, S. G., *Eur. J. Inorg. Chem.* **2016**, 432-438; b) Shatruk, M; Phan, H.; Chrisostomo, B. A.; Suleimenova; A., *Coord. Chem. Rev.* **2015**, *289-290*, 62-73; c) Brooker S., *Chem. Soc. Rev.* **2015**, *44*, 2880-2892; d) Halcrow, M. A.; Spin-Crossover Materials:

Properties and Applications, John Wiley & Sons (Eds.), **2013**; e) Gütlich, P.; Goodwin H. A. (Eds.), *Top. Curr. Chem.* **2004**, *233-235.*

(4) see for example: a) Gütlich, P.; Gaspar, A.-B.; Garcia, Y., *Beilstein J. Org. Chem.* **2013**, *9*, 342–391; b) Muñoz-Lara, F. J.; Arcís-Castillo, Z.; Muñoz, M.-C.; Rodríguez-Velamazán, J.-A.; Gaspar, A.-B.; Real, J.-A., *Inorg. Chem.* **2012**, *51*, 11126-11132; c) Olguin, J.; Brooker, S., *Coord. Chem. Rev.* **2011**, *255*, 203-240; d) Halcrow, M. A., *Chem. Soc. Rev.* **2011**, *40*, 4119-4142; e) Halcrow, M. A., *Coord. Chem. Rev.* **2009**, *253*, 2493-2514; f) Real, J.-A.; Gaspar, A.-B.; Niel, V.; Muñoz, M. C., *Coord. Chem. Rev.* **2003**, *236*, 121-141.

(5) a) Yamasaki, M.; Ishida, T., *Polyhedron* **2015**, *85*, 795-799; b) Hirosawa, N.; Oso, Y.; Ishida, T., *Chem. Lett.* **2012**, *41*, 716-718.

(6) Dupouy, G.; Marchivie, M.; Triki, S.; Sala-Pala, J.; Salaün, J. Y.; Gómez-García, C. J.; Guionneau, P., *Inorg. Chem.* **2008**, *47*, 8921-8931.

(7) a) Dupouy, G.; Marchivie, M.; Triki, S.; Sala-Pala, J.; Gomez-Garcia, C. J.; Pillet, S.; Lecomte, C.; Létard, J.-F., *Chem. Commun.* **2009**, 3404-3406; b) Dupouy, G.; Triki, S.; Marchivie, M.; Cosquer, N.; Gómez-García, C. J.; Pillet, S.; Bendeif, E.-E.; Lecomte, C.; Asthana, S.; Létard, J.-F., *Inorg. Chem*. **2010**, *49*, 9358-9368;

(8) a) Wei, R.-J.; Li, B.; Tao, J.; Huang, R.-B.; Zheng, L.-S.; Zheng, Z*., Inorg. Chem*. **2011**, *509*, 1170-1172; b) Højland, F.; Toftlund, H.; Yde-Anderson, S., *Acta Chem. Scand.* **1983**, *A37*, 251-257; c) Paulsen, H.; Grünsteudel, H.; Meyer-Klaucke, W.; Gerdan, M.; Grünsteudel, H. F.; Chumakov, A. I.; Rüffer, R.; Winkler, H.; Toftlund, H.; Trautwein, A. X., *Eur. Phys. J.* **2001**, *B23*, 463-472; d) Li, B.; Wei, R.-J.; Tao, J.; Huang, R.-B.; Zheng, L.-S.; Zheng, Z., *J. Am. Chem. Soc.* **2010**, *132*, 1558-1566.

(9) Wei, R.-J.; Huo, Q.; Tao, J.; Huang, R.-B.; Zheng, L.-S., *Angew. Chem. Int. Ed.* **2011***, 50,* 8940-8943.

(10) Park, J. G.; Jeon, I.-R.; Harris, T. D., *Inorg. Chem. **2015**, 54,* 359-369.

(11) a) Gaspar, A. B.; Ksenofontov, V.; Real, J. A.; Gütlich, P., *Chem. Phys. Let.* **200**3, *373*, 385-391; b) Gaspar A. B.; Ksenofontov, V.; Martinez, V.; Real, J. A.; Gütlich, P., *Eur. J. Inorg. Chem.* **200**4, 4770-4773; c) Gaspar, A. B.; Muñoz, M.-C.; Real, J. A., *J. Mater. Chem.* **2005**, *16*, 2522-2533.

(12) Ksenofontov, V.; Gaspar, A. B.; Niel, V.; Reiman, S.; Real, J. A.; Gütlich, P., *Chem. Eur. J.* **200**4, *10*, 1291-1298

(13) a) Hogue, R. W.; Feltham, H. L. C.; Miller, R. G.; Brooker, S., *Inorg. Chem.* **2016**, *55*, 4152–4165; b) Herold, C. F.; Carrella, L. M.; Rentschler, E., *Eur. J. Inog. Chem.* **2015**, 3632-3636; c) Kulmaczewski, R.; Olguín, J.; Kitchen, J. A.; Feltham, H. L. C.; Jameson, G. N. L.;

Tallon, J. L.; Brooker, S., *J. Am. Chem. Soc.* **2014**, *136*, 878–881; d) Kitchen, J. A.; Oluín, J.; Kulmaczewski, R.; White, N. G.; Milway, V. A.; Jameson, G. N. L.; Tallon, J. L.; Brooker, S., *Inorg. Chem.* **2013**, *52*, 11185–11199; e) Kitchen, J. A.; White, N. G.; Jameson, G. N. L.; Tallon; J. L.; Brooker, S., *Inorg. Chem.* **2011**, *50*, 4586–4597; f) Grunert, C. M.; Reiman, S.; Spiering, H.; Kitchen, J. A.; Brooker, S.; Gütlich, P., *Angew. Chem. Int. Ed.* **2008**, *47*, 2997–2999; g) Klingele, M. H.; Moubaraki, B.; Murray, K. S.; Brooker, S., *Chem. Eur. J.* **2005**, *11*, 6962–6973; h) Klingele, M. H.; Moubaraki, B.; Cashion, J. D.; Murray, K. S.; Brooker, S., *Chem. Commun.* **2005**, 987–989; i) Nakano, K.; Suemura, N.; Yoneda, K.; Kawata, S.; Kaizaki, S., *Dalton Trans.* **2005**, 740-743; j) Leita, B. A.; Moubaraki, B.; Murray, K. S.; Smith, J. P.; Cashion, J. D., *Chem. Commun.* **2004**, 156–157; k) Nakano, K.; Kawata, S.; Yoneda, K.; Fuyuhiro, A.; Yagi, T.; Nasu, S.; Morimoto, S.; Kaizaki, S., *Chem. Commun.* **2004**, 2892–2893.

(14) Ortega-Villar, N.; Thompson, A.-L.;Muñoz, M.-C; Ugalde-Saldivar; Goeta, A. E.; Moreno-Esparza, R.; Real, J. A., *Chem. Eur. J.* **200**5, *110*, 5721-5734.

(15) Burdette, S. C.; Frederickson, C. J.; Bu, W.; Lippard, S. J., *J. Am. Chem. Soc.* **2003**, *125*, 1778-1787.

(16) Schlager, O.; Wieghardt, K.; Grondey, H.; Rufinska, A.; Nuber, B., *Inorg. Chem.* **1995**, *34*, 6440-6448.

(17) Roger, M.; Patinec, V.; Tripier, R.; Triki, S.; Le Poul, N.; Le Mest, Y., *Inorg. Chim. Acta*, **2014**, *417*, 201-207.

(18) Elemental analyses have been performed on single crystals of **1.MeOH** and **1** (obtained by heating **1** at 70 °C during three hours). However the values found for C, H and N atoms did not show significant difference between the two analyses. The fraction of 0.3 MeOH calculated from the elemental analysis of **1.MeOH**, should be considered as the maximum value. This observation implies that the loss of solvent molecules occurs easily before the analysis.

(19) a) Darawsheh, M.; Barrios, L. A.; Roubeau, O.; Teat, S. J.; Aromi, G., *Chem. Eur. J.* **2016**, *22*, 8635-8645; b) Amoore, J. J. M.; Kepert, C. J.; Cashion, J. D.; Moubaraki, B.; Neville, S.; Murray, K. S., *Chem. Eur. J.* **2006**, *12*, 8220-8227; c) Amoore, J. J. M.; Neville, S. M.; Moubaraki, B.; Iremonger, S. S.; Murray, K. S.; Létard, J.-F.; Kepert, C. J., *Chem. Eur. J.* **2010**, *16*, 1973-1982; d) Matouzenko, G. S.; Jeanneau, E.; Verat, A. Y.; de Gaetano, Y., *Eur. J. Inorg. Chem*. **2012**, 969-977.

(20) See for examples: Olguin, J.; Brooker, S. in *Spin-Crossover Materials: Properties and Applications*, Ed. Halcrow M.A. 2013 John Wiley & sons, 77-120.

(21) a) Bousseksou, A.; Nasser, J.; Linares, J.; Boukheddaden, K.; Varret, F., *J. Phys. I* **1992**, *2*, 1381−1403; b) Bousseksou, A.; Varret, F.; Nasser, J., *J. Phys. I* **1993**, *3*, 1463−1473; c) Boukheddaden, K.; Linares, J.; Codjovi, E.; Varret, F.; Niel, V.; Real, J. A., *J. Appl. Phys.* **2003**, *93*, 7103-7105; d) Nishino, M.; Boukheddaden, K.; Miyashita, S.; Varret, F., *Phys. Rev. B* **2003**, *68*, 224402; e) Paez-Espejo, M.; Sy, M.; boukheddaden, K., *J. Am. Chem. Soc.* **2016**, *138*, 3202-3210.

(22) Kaiba, A.; Shepherd, H. J.; Fedaoui, D.; Rosa, P.; Goeta, A. E.; Rebbani, N.; Létard, J.-F.; Guionneau, P., *Dalton Trans.* **2010**, *39*, 2910-2918.

(23) Deeney, F. A.; Harding, C. J.; Morgan, G. G.; McKee, V.; Nelson, J.; Teat, S. J.; Clegg, W., *Dalton Trans.* **1998**, 1837-1844.

(24) Guionneau, P.; Marchivie, M.; Bravic, G.; Létard, J.-F. D. Chasseau, *Top. Curr. Chem.,* **2004** *234*, 97-128.

(25) Marchivie, M.; Guionneau, P.; Létard, J.-F.; Chasseau, D., *Acta Cryst. B* **2005,** *B61*, 25-28.

(26) J. Tao, J.; Wei,R.-J.; Huang, R.-B.; Zheng, L.-S., *Chem. Soc. Rev.* **2012**, *41*, 703–737.

(27) Middleton, W. J.; Little, E. L.; Coffman, D. D.; Engelhardt, V. A., *J. Am. Chem. Soc.* **1958**, *80*, 2795-2809.

(28) Britovsek, G. J. P.; England, J.; White, A. J. P., *Inorg.Chem*. **2005**, *44*, 8125-8134.

(29) Bain, G. A.; Berry, J. F., *J. Chem. Educ.* **2008**, *85*, 532-536.

(30) *CRYSALIS-CCD 170*, Oxford-Diffraction, **2002**; *CRYSALIS-RED 170*, Oxford-Diffraction, **2002**.

(31) Sheldrick, M. SHELX97, *Program for Crystal Structure Analysis*, University of Gottingen, Gottingen, Germany, **1997**.

(32) Farrugia, L. J., *J. Appl. Crystallogr.* **1999**, *32*, 837-838.

(33) Dolomanov, O. V.; Bourhis, L. J.; Gildea, R. J.; Howard, J. A. K.; Puschmann, H., *J. Appl. Cryst.*, **2009**, *42*, 339-341.

Synopsis and structural diagram

Dinuclear Spin Cross-Over Complexes Based on Tetradentate and Bridging Cyanocarbanion Ligands.

Eric Milin, Sabrina Belaïd, Véronique Patinec, Smail Triki, Guillaume Chastanet, Mathieu Marchivie

New Fe^{II} dinuclear neutral complexes of formula $[Fe_2(L)_2(\mu_2\text{-tcpd})_2]\bullet nCH_3OH$ (L = tmpa = tris(2-pyridylmethyl)amine (**1.MeOH**, **1**); L = andmpa = bis-(2-pyridylmethyl)aminomethyl)aniline (**2.MeOH**); $(tcpd)^{2-}$ = 2-dicyanomethylene-1,1,3,3-tetracyanopropanediide anion, n = 0.8 for **1.MeOH**, 0 for **1**, and 2 for **2.MeOH**) have been synthesized and structurally characterized. Detailed structural and magnetic studies are in agreement with the presence one-step spin crossover (*SCO*) behaviors in these complexes.